Physics of the Earth and Planetary Interiors 180 (2010) 148–153

Contents lists available at ScienceDirect

Physics of the Earth and Planetary Interiors

journal homepage: www.elsevier.com/locate/pepi

Effect of composition, structure, and spin state on the thermal conductivity of the Earth's lower mantle

A.F. Goncharov[a,*], V.V. Struzhkin[a], J.A. Montoya[a], S. Kharlamova[a], R. Kundargi[a], J. Siebert[b,c], J. Badro[b,c], D. Antonangeli[b,c], F.J. Ryerson[c], W. Mao[d,e]

[a] Geophysical Laboratory, Carnegie Institution of Washington, Washington, DC 20015, United States
[b] Institut de Minéralogie et de Physique des Milieux Condensés, UMR CNRS 7590, Institut de Physique du Globe de Paris, Université Pierre et Marie Curie, France
[c] Lawrence Livermore National Laboratory, Livermore, CA 94550, United States
[d] Geological and Environmental Sciences, Stanford University, Stanford, CA 94305, United States
[e] Photon Science, SLAC National Accelerator Laboratory, Menlo Park, CA 94025, United States

ARTICLE INFO

Article history:
Received 31 May 2009
Received in revised form 20 January 2010
Accepted 1 February 2010

Guest Editors
Kei Hirose
Thorne Lay
David Yuen

Editor
G. Helffrich

Keywords:
Thermal conductivity
Lower mantle
Iron bearing Earth's minerals
Electronic spin transition
High pressure
Optical properties
Diamond anvil cell

ABSTRACT

The change in electronic structure of iron at high pressures to spin-paired states in ferropericlase, silicate perovskite, and post-perovskite may have a profound influence on the thermal conductivity of the lower mantle. Here, we present optical absorption data for lower mantle minerals to assess the effect of composition (including iron oxidation state), structure, and iron spin state on radiative heat transfer. We confirm that the presence of ferric iron in ferropericlase strongly affects the optical properties, while the effect of the spin-pairing transition may be more secondary. We also show that post-perovskite exhibits larger optical absorption in the near infrared and visible spectral ranges than perovskite which may have a profound effect on the dynamics the lowermost mantle. We present preliminary results from measurements of the phonon thermal conductivity of perovskite at 125 GPa using a pulsed laser heating technique. The available data suggest a larger value than what previously estimated, although the uncertainty is large.

1. Introduction

Knowledge of thermal conductivity of lower mantle materials is of critical importance for understanding of the Earth's thermal structure, evolution, and dynamics. Heat fluxes through the Earth's mantle depend on the thermal conductivity of constituent minerals. Mantle convection and plate tectonics are largely dependent on these heat fluxes. Thermal conductivity values may change dramatically due to spin crossover which can profoundly affect the electronic properties of Fe-bearing lower mantle minerals (Sherman, 1991; Burns, 1993; Badro et al., 2003). It has been suggested that radiative thermal conductivity might increase at the spin-pairing transition due to the loss of the IR absorption band corresponding to the crystal-field transition (Sherman, 1991; Badro et al., 2004). The open discussion on the spin state of the materials making up the lower mantle, the debate on the exact nature of the spin state in post-perovskite (mixed versus intermediate (Lin et al., 2008)), and the complex mechanisms contributing to the optical absorption (Goncharov et al., 2006) call for additional investigations on the effects of spin transition phenomena on the Earth's radiative thermal conductivity. Moreover, the effect of the spin transition on the phonon component of the thermal conductivity is largely unconstrained.

Determination of optical and phonon heat transfer at high pressure and high temperature is a challenging task that has been addressed through a variety of approaches, including direct experimental measurements, extrapolations of lower pressure–temperature data, and theoretical calculations. So far, there are few theoretical calculations (Cohen, 1998), and their accuracy has not been assessed. Extrapolation of the lower pressure–temperature data based on empirical relations (Hofmeister, 1999) can serve as a first approximation, but will not

* Corresponding author. Tel.: +1 202 478 8947.
E-mail address: goncharov@gl.ciw.edu (A.F. Goncharov).

0031-9201/$ – see front matter © 2010 Elsevier B.V. All rights reserved.
doi:10.1016/j.pepi.2010.02.002

work when the effect of spin transitions need to be taken into account.

Here we present the results from a series of experiments in the diamond anvil cell (DAC) on the radiative and phonon thermal conductivity of the major phases of the lower mantle (*i.e.* Fe, Mg silicate perovskite, post-perovskite, and ferropericlase) and assess the effects of spin state, composition, and structure. In the case of ferropericlase, we focus on samples with very low ferric iron content, as more representative for the oxygen fugacity conditions (fO_2) of the lower mantle (Keppler et al., 2007). We compare the radiative thermal conductivity of perovskite and post-perovskite to directly evaluate if this structural transition is ultimately driving the radiative thermal conductivity in the lowermost mantle rather than the change in the spin state as suggested by recent X-ray synchrotron measurements (Lin et al., 2008).

2. Experimental procedure

2.1. Sample synthesis

Oriented single crystals of ferropericlase, $Fe_xMg_{(1-x)}O$, were synthesized starting from a pre-aligned crystal of MgO (normal parallel to [1 1 0] direction) by high-temperature Fe–Mg interdiffusion in a piston cylinder press (1400 °C at 1 GPa for 200 h). The oxygen fugacity was buffered close to the IW (Iron-Wüstite) buffer by loading the sample in an iron capsule. A 40 nm thick focused ion beam section was cut out of the recovered sample for electron energy loss spectroscopy measurement, and no detectable amount of ferric iron was measured. Samples with total iron content $\leq 25\%$ prepared at ambient pressure close to the IW buffer can have up to 2% $Fe^{3+}/\sum Fe$ (Srecec et al., 1987). Since high pressure is known to destabilize Fe^{3+}, this estimation can be reasonably considered as upper limit for our samples, synthesized at 1 GPa. The samples were polished to 8–20 μm thickness and cut to approximately 40 μm in diameter. We produced samples with different iron content x, varying in the 0.15–0.21 range; the exact composition was determined individually for each disk by electron microprobe analysis.

Samples of perovskite, $Fe_{0.1}Mg_{0.9}SiO_3$, were synthesized under high pressure (125 GPa) in a laser heated DAC using an orthopyroxene starting material. To couple the laser heating radiation with the sample, a small Ir square (called coupler below) of 20 μm × 20 μm × 5 μm was positioned in the middle of a cavity filled by the sample on all sides. Thin 1–2 μm alumina thermal insulation layers were deposited on the diamond anvils (Goncharov et al., 2008a,b). The X-ray diffraction measurements performed after the laser heating showed that the material synthesized was predominantly in the perovskite phase (a trace amount of post-perovskite was also detected).

Samples of post-perovskite, $Fe_xMg_{(1-x)}SiO_3$ were also synthesized under high pressure (>135 GPa) in a laser heated DAC using an orthopyroxene starting material (Mao et al., 2004). X-ray diffraction showed that the sample was single phase post-perovskite. The iron content, x, ranged from 0.1 to 0.3 in the samples studied (samples with larger x were essentially opaque over the entire spectral range). The sample with low Fe concentration ($x = 0.1$), which was partially transparent in the visible, looked optically uniform when observed using an optical microscope in transmitted light. Thus, we believe that possible effects of light scattering on the intergrain boundaries on the optical absorption spectra are small.

2.2. Optical measurements

Our experimental methods for determination of the phonon and radiative thermal conductivity in the DAC are described elsewhere (Goncharov et al., 2006; Beck et al., 2007; Goncharov et al., 2009). Here we explore various possibilities in sample preparation and reaching higher pressures to address the dependence of composition, structure, and electronic state on the thermal conductivity. Similarly to the previous publications (Goncharov et al., 2006, 2008a,b, 2009; Keppler et al., 2007, 2008), we assessed the radiative thermal conductivity based on the measurements of the optical absorption spectra assuming that the grain size is larger than the typical absorption length (*e.g.*, Hofmeister, 2005).

Optical absorption spectra of ferropericlase were measured using Ne as a pressure medium. As in our previous studies (Goncharov et al., 2006, 2008a,b, 2009), the sample absorbance was determined by referencing to a spectrum measured at the same pressure through the pressure medium. The sample thickness was determined at ambient pressure by using optical interferometry (in reflection spectra), and calculated at high pressure using an isothermal equation of state.

Optical absorption spectra of post-perovskite were normalized to the transmission spectra of the optical system without the DAC, and the diamond absorption was taken into account from the separate measurements of the diamond anvils. The sample thickness was estimated for the sample with $x = 0.1$ using reflectivity measurements of the sample portion containing only the thermal insulation (NaCl). The sample thickness was assumed to be the same for the other samples since the diamond culet dimensions and pressure were almost the same. All the optical absorption measurements reported here were performed at room temperature.

The overall uncertainty in determination of the absorption coefficient, $k = (\log I_0/\log I)\ln 10/d$ can be estimated as follows. The accuracy of the absorbance measurements $A = \log I_0/\log I$ are mainly due to baseline-to-sample measurement uncertainties, caused by sample and cavity imperfections and limited sample dimensions. These are normally within $\Delta A = 0.1$ based on random errors obtained from several measurements. The accuracy of the determination of the sample thickness (assuming non-deformed samples in a medium) are mainly determined by the uncertainty in the equation of state and related to this pressure measurement uncertainty, and by the initial thickness determination errors. These combined errors do not exceed 1%. Based on the above discussion, we conclude that the experimental uncertainty of the absorption coefficient is determined by the experimental factors limiting the accuracy of the absorbance measurements. For the typical sample thicknesses (<15 μm), the uncertainty in k is about 50 cm^{-1} (see also Goncharov et al., 2008a,b). The uncertainties in determination of the absorption coefficient in the case of post-perovskite samples are larger (up to 20%) since the sample thickness could only be approximately estimated as described above.

3. Results and discussions

3.1. Ferropericlase

Absorption measurements in ferropericlase with $x = 0.204$ to pressures up to 36 GPa show a monotonic increase of absorption in the high-spin state (Fig. 1). This is in contrast to the results of Keppler et al. (2007), who did not observe any systematic increase in the background intensity for their sample with $x = 0.12$ synthesized under high pressure. Our data at low pressures ($\leq$5 GPa) are in qualitative agreement with those of Keppler et al. (2007) (Fig. 1a); thus the difference in high-pressure behavior is not due to differences in sample preparation procedures. We determined the sample thickness at 0 GPa to be approximately 16 μm by measuring the interference fringes in transmission spectra in the near IR and visible spectral ranges. The absorption coefficient of ferropericlase determined from these measurements is lower than the value

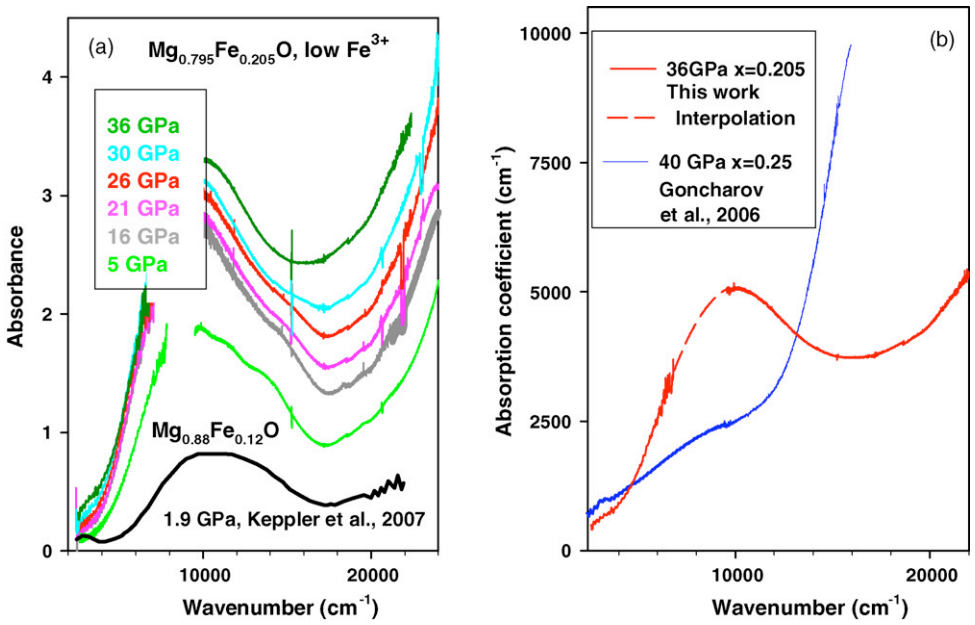

Fig. 1. Optical absorption spectra of ferropericlase $Mg_{(1-x)}Fe_xO$. (a) Pressure dependence of absorbance of sample with a low ferric iron concentration from this work ($x = 0.205$). Black solid curve – data at 1.9 GPa from the work of Keppler et al. (2007) for the sample of different thickness and different iron content ($x = 0.12$). (b) Comparison of the 36 GPa absorption coefficient spectrum from this work with that determined by Goncharov et al. (2006) for another sample batch. The absorption coefficient has been calculated using $k = A \ln 10/d$, where $A = \log_{10}(I_0/I)$ is the absorbance, d is the sample thickness (see text).

determined by Goncharov et al. (2006) in the visible and ultraviolet (UV), but it is larger in the near IR range (Fig. 1b). These measurements show that samples with higher Fe^{3+} content (as presumably was the case for the samples used in the study of Goncharov et al. (2006)) do have substantial additional absorption in the visible and UV due to charge transfer bands. Nevertheless, even samples with no measurable amount of ferric iron, show a background absorption in the visible and a gap-like increase of absorption in the UV (Fig. 1), see also Keppler et al. (2007). Preliminary results from absorption measurements at higher pressures across the spin transition show trends similar to what was reported by Goncharov et al. (2006) and Keppler et al. (2007) – *i.e.* no major reduction of the absorption in the near IR at the transition. Since this spectral range corresponds to the maximum in blackbody emission for temperatures between 2000 and 3000 K (970 nm at 3000 K), we conclude that the iron oxidation state has larger effects on the radiative conductivity in ferropericlase than the changes in the spin state, and thus, is to going to play a major role in the thermal conductivity of the Earth's lower mantle.

3.2. Silicate perovskite

Direct measurements of the optical absorption in silicate perovskite (Goncharov et al., 2008a,b; Keppler et al., 2008) show that the effect of spin transition at 30–70 GPa (Badro et al., 2004) on the optical absorption is very small. Goncharov et al. (2008a,b) observed a gradual decrease of intensity of the Fe^{2+} crystal-field band around 50 GPa, which may be related to the spin pairing of ferrous iron. The high-pressure low-spin state (called "intermediate" in recent publications (Lin et al., 2008; McCammon et al., 2008)) corresponds to the spin-paired state ($S = 1$) one expects in the case of a distorted dodecahedral site occupied by Fe^{2+} in perovskite (*e.g.*, Burns, 1993).

3.3. Post-perovskite

Surprisingly, our absorption spectra of post-perovskite at 140 GPa (Fig. 2) show a strong band at 12,000 cm^{-1}. This is close in frequency to the crystal-field transition at high pressures (the transition normally blue-shifts with pressure in ferropericlase (Goncharov et al., 2006) and perovskite (Goncharov et al., 2008a,b)). The spectra of post-perovskite with different Fe content are qualitatively similar; they differ quantitatively in the absorption coefficient, which shows, as expected, an increase with the iron content. Samples with higher Fe content also show the absorption band near 8000 cm^{-1}, which falls within a characteristic spectral range of the crystal-field transition of Fe^{2+}. This result suggests that the spin state of Fe in post-perovskite can be more complex than previously suggested (Lin et al., 2008). Moreover, the comparison of the absorption spectra of perovskite and post-perovskite with

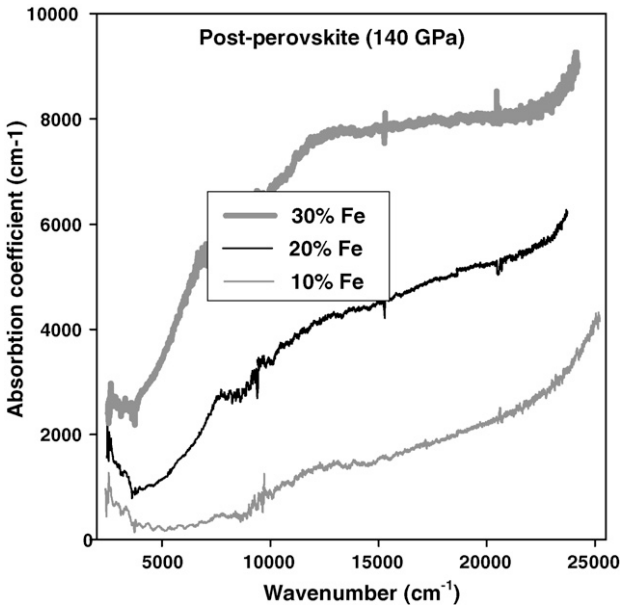

Fig. 2. Optical absorption spectra of post-perosvskite with different iron compositions. The absorption coefficient has been determined as described in the caption to Fig. 1. The sample thickness was estimated to be 5.75 μm (see text).

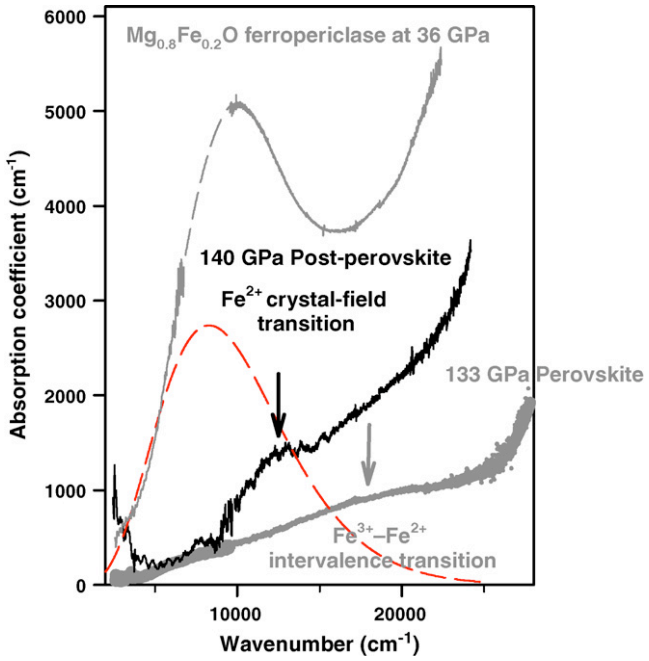

Fig. 3. Comparison of the optical absorption spectra of post-perovskite, ferropericlase (this work), and perovskite from work of Goncharov et al. (2008a,b). The dashed (red) line represents the calculated blackbody radiation (arbitrary units) at 2400 K, close to lower mantle conditions. (For interpretation of the references to color in this figure legend, the reader is referred to the web version of the article.)

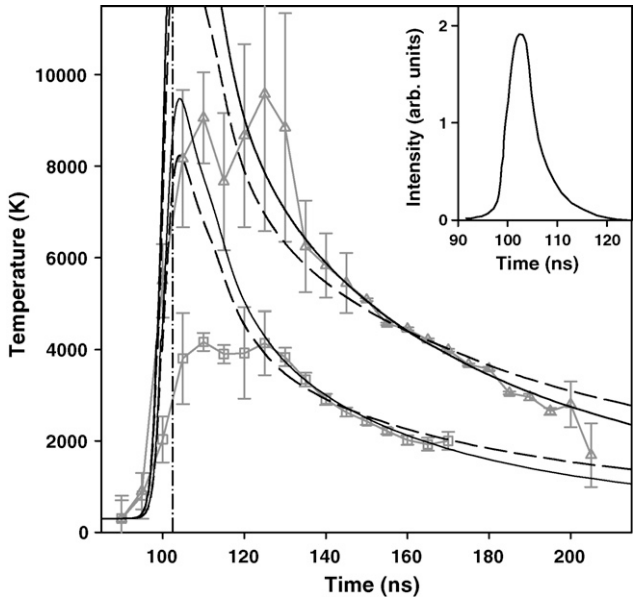

Fig. 4. Time dependence of surface temperature of the Ir foil imbedded into perovskite sample at 125 GPa. The two datasets are for different pulse energies. Symbols with error bars – spectroradiometric measurements, solid lines – FE calculations with $k_{300\,K}$ = 100 W/mK, dashed lines – same with $k_{300\,K}$ = 30 W/mK. Vertical dot-dashed line corresponds to the maximum of the laser pulse. Inset – the laser pulse profile.

x = 0.1 at similar conditions (Fig. 3) shows that post-perovskite has a larger absorption coefficient in the near IR-visible-UV spectral range and, hence, smaller radiative conductivity than perovskite. This is consistent with recent observations of an increased electrical conductivity of post-perovskite (Ohta et al., 2008). No pressure dependence of the absorption spectra for perovskite could be measured in this work due to technical reasons. Further studies are needed to explain the effects of the spin transition on the radiative thermal conductivity. Unfortunately, the measurements of the pressure dependence are limited because of the structural instability of post-perovskite upon pressure release.

3.4. Lattice thermal conductivity of silicate perovskite

Measurements of the phonon thermal conductivity using a ns pulsed laser heating technique combined with time-resolved radiometry proposed by Beck et al. (2007) require the use of a very thin (<0.1 μm thick) coupler, which is difficult to bring intact to ultrahigh pressures. Here we present the results of a feasibility study using a thicker coupler (see also Kundargi et al., 2008). The experimental time-dependent measurements of the coupler surface temperature (Fig. 4) show an abrupt increase in temperature after the laser pulse arrival followed by a slower cooling cycle. It is interesting to note that in contrast to the results of Beck et al. (2007), we find that the temperature of the coupler remains approximately constant for a time period of about 25 ns at the maximum of the temperature-time dependences (Fig. 4). Measurements with different pulse energies show qualitatively similar curves; thus the effects related to melting phenomena (both coupler and sample are expected to melt in the 4000–5000 K temperature range based on measurements reported in Errandonea et al., 2001; Kavner and Jeanloz, 1998; Zerr and Boehler, 1993) should be ruled out. Examination of the incandescent spectra near the top of the temperature-times curve show large departures from Planck's law. We attribute these departures to essentially nonequilibrium heat transfer processes in the coupler (see Chen, 1996), which occur during and shortly after the arrival of the laser pulse. The effects related to radiative cooling (governed by the Stefan–Bolzmann's law) are negligible at the temperatures measured here (<10,000 K) (*e.g.*, Beck et al., 2007, 2009).

In order to extract the thermal conductivity of the perovskite sample we applied finite-element (FE) calculations to solve the heat-flow diffusion equation (see Crank, 1967 for details) in a cavity of the DAC (see also previous publications: Bodea and Jeanloz, 1989; Dewaele et al., 1998; Kiefer and Duffy, 2005). We used a FLEX PDE 3D professional software package along with a code we developed specifically for analysis of time-dependent heat fluxes in the DAC (Montoya et al., in preparation). The thermochemical parameters of material in the DAC cavity were taken from the literature and scaled to the pressure conditions of the observations (125 GPa) using the scaling relations available from literature (Ross et al., 1984). We assumed that the thermal conductivity of perovskite depends on temperature as $T^{1/2}$ as proposed in Klemens (1960) and measured for other silicates by Xu et al. (2004). More complex temperature dependences would not be required by our data. These parameters and the scaling relation are presented in Table 1. As in the previous work (Kiefer and Duffy, 2005) a sufficient portion of diamond anvils was included into the simulation domain (20 μm thickness); the results did not significantly alter when a larger thickness was included.

The results of our FE calculations for the time dependence of the surface temperature of the coupler compare well with the experiment except for the region at top of the curve (Fig. 4). In this range the calculations give much higher temperatures while the spectroradiometric measurements show a "plateau". One possible explanation is that our FE calculations use a classic formalism to solve the heat conduction problem at the interface neglecting the presence of this absorbing layer, while the Ir coupler has a small but finite optical depth (we estimated it to be 13 nm at 1064 nm wavelength using the experimental data of Lehmuskero et al. (2007)). Thus, unlike for the model assumptions, a non-negligible amount of the laser radiation is absorbed in the depth of the coupler which reduces the effective surface temperature. After the entire laser

Table 1
Thermochemical parameters of materials used in FE calculations.

Property/material	Diamond	Sample	Coupler (Ir) (Cargan and Pottlacher, 2007)
Density (kg/m^3)	3,500	5,168	27,136
Thermal conductivity (W/mK)	2,000	$k_{300\,K}(300/T)^{1/2}$	$300(1-8.4\times10^{-5}\,(T-300))\;T<4200$ $150(1+21\times10^{-5}(T-4200))\;T>4200$
Specific heat capacity (J/kg K)	509	1,400	$(136.22-0.0361T+5.60875\times10^{-5}T^2-1.5532\times10^{-8}T^3+1.3170\times10^{-12}T^4)\;T<4200$; 233 $T>4200$
Emisivity	0	0	0.55 $T<4200$; 0.35 $T>4200$

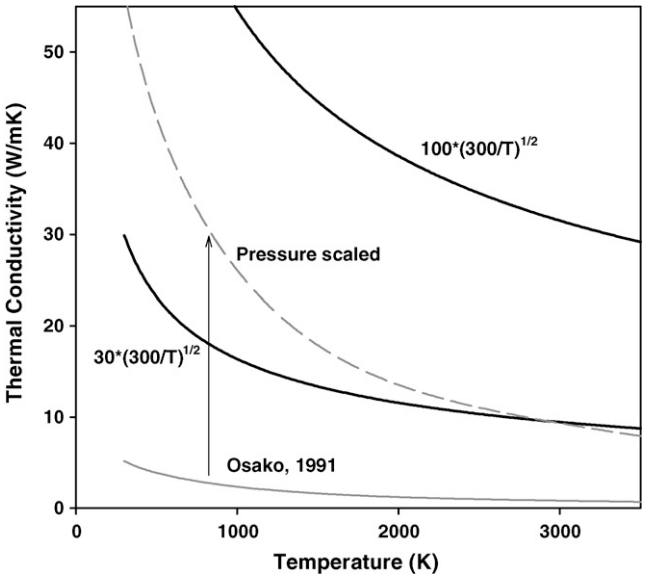

Fig. 5. Thermal conductivity of perovskite as a function of temperature. Solid gray line – ambient pressure data from Osako (1991). Dashed gray line – extrapolation to 125 GPa data of Osako (1991) using an empirical relation $k=k_0(V_0/V)^7$, where zero subscript refers to ambient pressure (Manga and Jeanloz, 1997). Thick bold lines represent the temperature dependences of the thermal conductivity used in the FE calculation in this work.

pulse is absorbed, the temperature distribution is governed by classic heat conduction laws, and our FE calculations become accurate in the part concerning the temperature distribution across the sample. For very thin couplers (0.1 μm) used in the previous work (Beck et al., 2007), the thermalization time after the laser pulse arrival was very short (0.25 ns), and hence the effect of nonequilibrium heat transfer becomes unobservable in the experiment.

We attempted to fit the whole experimental data with a single set of thermochemical parameters, leaving laser pulse energy as a free parameter for fitting. Our FE calculations approximate well the experimental temperature–time curves obtained with different laser pulse energies (and hence to different temperatures). Unfortunately, in the present experimental configuration the temperature–time curves are less dependent on the thermal conductivity of the sample than they are on the thermal properties of the coupler. Thus, our measurements can only determine the thermal conductivity of the sample with a large uncertainty. Our results are illustrated in Fig. 5 along with previous estimates based on ambient pressure measurements (Osako, 1991) and extrapolation to higher pressures (Manga and Jeanloz, 1997). Previous determinations of the thermal conductivity of perovskite under the lower mantle conditions (Osako, 1991) predict a value of 12 W m^{-1} K^{-1} at the top of D" layer (2500 K). Our best estimate (Fig. 5) is slightly higher, but agrees within the uncertainty.

4. Conclusions

We present a suite of experimental results aimed at ultimately determining the thermal conductivity of the main phases in the Earth's lower mantle. Optical absorption spectra of lower mantle minerals depend critically on composition (including iron oxidation state), structure, and iron spin state. We confirm that the presence of ferric iron in ferropericlase strongly affects the optical properties. We also show that perovskite and post-perovskite exhibit substantially different optical absorption in the near infrared and visible spectral ranges (cf., the results of Lin et al., 2008); this may have a profound effect on the dynamics the lowermost mantle. Simultaneous effects of pressure and temperature on the optical properties still remain largely unknown. Further work is required for an accurate assessment of the radiative component of the thermal conductivity of lower mantle minerals, including the study of compositional and structural properties, as well as the iron spin state.

Preliminary results from measurements of the phonon thermal conductivity of perovskite at 125 GPa using a pulsed laser heating technique suggest a larger value than what was previously estimated, although the uncertainty is very large. Future accurate experimental measurements of the phonon contribution to the thermal conductivity of lower mantle materials will require a number of carefully crafted experiments under high pressure and temperature conditions to determine the thermal conductivity of all the materials used in the DAC. Thin couplers prepared as metallic films directly deposited on mineral plates should be used in next generation pulsed laser heating experiments, and the first tests are currently underway.

Acknowledgements

We acknowledge support from NSF EAR 0711358 and 0738873, Carnegie Institution of Washington, DOE/BES, DOE/NNSA (CDAC), and the W.M. Keck Foundation. We wish to thank C. Aracne for her help in the thinning and cutting of the ferropericlase samples. We thank P. Lazor and Z. Konopkova for introducing us to the finite-element calculations. J. B. acknowledges support by the French National Research Agency (ANR) grant no. ANR-07-BLAN-0124-01. R.K. was supported by the NSF Research Experience for Undergraduates (REU) Program at the Carnegie Institution of Washington. Use of the HPCAT facility (Carnegie Institution of Washington) was supported by DOE-BES, DOE-NNSA (CDAC), NSF, DOD-TACOM and the W.M. Keck Foundation. Use of the Advanced Photon Source was supported by the US Department of Energy, Office of Science, Office of Basic Energy Sciences, under Contract No. W-31-109-Eng-38. We thank Y. Meng for help with X-ray diffraction experiments in the laser heated DAC.

References

Badro, J., Fiquet, G., Guyot, F., Struzhkin, V.V., Rueff, J.-P., Vanko, G., Monaco, G., 2003. Iron partitioning in Earth's mantle: toward a deep lower mantle discontinuity. Science 300, 789–791.

Badro, J., Rueff, J.-P., Vanko, G., Monaco, G., Fiquet, G., Guyot, F., 2004. Electronic transitions in perovskite: possible nonconvecting layers in the lower mantle. Science 305, 383–386.

Beck, P., Goncharov, A.F., Struzhkin, V., Militzer, B., Mao, H.-K., Hemley, R.J., 2007. Measurement of thermal diffusivity at high pressure using a transient heating technique. Appl. Phys. Lett. 91, 181914-(1–3).

Beck, P., Goncharov, A.F., Montoya, J.A., Struzhkin, V.V., Militzer, B., Hemley, R.J., Mao, H.-K., 2009. Response to "Comment on 'Measurement of thermal diffusivity at

high-pressure using a transient heating technique". Appl. Phys. Lett. 95, 096101-(1–2).
Bodea, S., Jeanloz, R., 1989. Model calculations of the temperature distributions in the laser heated diamond cell. J. Appl. Phys. 65, 4688–4692.
Burns, R.G., 1993. Mineralogical Applications of Crystal Field Theory, 2nd ed. Cambridge University Press, Cambridge, UK.
Cargan, C., Pottlacher, G., 2007. Thermodynamic properties and normal spectral emittance of iridium up to 3500 K. Int. J. Thermodyn. 28, 697–710.
Chen, G., 1996. Nonlocal and nonequilibrium heat conduction in the vicinity of nanoparticles. J. Heat Transfer 118, 539 (1–7).
Crank, J., 1967. The Mathematics of Diffusion. Oxford University Press, London, p. 347.
Cohen, R.E., 1998. Thermal conductivity of MgO at high pressures. Proceedings of the AIRAPT16. Rev. High Pressure Sci. Technol. 7, 160–162.
Dewaele, A., Fiquet, G., Gillet, P., 1998. Temperature and pressure distribution in the laser-heated diamond–anvil cell. Rev. Sci. Instrum. 69, 2421–2426.
Errandonea, D., Schwager, B., Ditz, R., Gessmann, C., Boehler, R., Ross, M., 2001. Systematics of transition-metal melting. Phys. Rev. B 63, 132104-(1–4).
Goncharov, A.F., Struzhkin, V.V., Jacobsen, S.D., 2006. Reduced radiative conductivity of low-spin (Mg, Fe)O in the lower mantle. Science 312, 1205–1208.
Goncharov, A.F., Beck, P., Struzhkin, V.V., Hemley, R.J., Crowhurst, J.C., 2008a. Laser heating diamond anvil cell studies of simple molecular systems at high pressures and temperatures. J. Phys. Chem. Solids 69, 2217–2222.
Goncharov, A.F., Haugen, B.D., Struzhkin, V.V., Beck, P., Jacobsen, S.D., 2008b. Radiative conductivity in the Earth's lower mantle. Nature 456, 231–234.
Goncharov, A.F., Beck, P., Struzhkin, V.V., Haugen, B.D., Jacobsen, S.D., 2009. Thermal conductivity of lower-mantle minerals. Phys. Earth Planet. Interior 174, 24–32.
Hofmeister, A.M., 1999. Mantle values of thermal conductivity and the geotherm from phonon lifetimes. Science 283, 1699–1706.
Hofmeister, A.M., 2005. Dependence of diffusive radiative transfer on grain-size, temperature, and Fe-content: implications for mantle processes. J. Geodyn. 40, 51–72.
Kavner, A., Jeanloz, R., 1998. High-pressure melting curve of platinum. J. Appl. Phys. 83, 7553–7559.
Keppler, H., Kantor, I., Dubrovinsky, L.S., 2007. Optical absorption spectra of ferropericlase to 84 GPa. Am. Mineral. 92, 433–436.
Keppler, H., Dubrovinsky, L.S., Narygina, O., Kantor, I., 2008. Optical absorption and radiative thermal conductivity of silicate perovskite to 125 GPa. Science 322, 1529–1532.
Klemens, P.G., 1960. Thermal resistance due to point defects at high temperatures. Phys. Rev. 119, 507–509.
Kiefer, B., Duffy, T.S., 2005. Finite element simulations of the laser-heated diamond–anvil cell. J. Appl. Phys. 97, 114902-(1–9).
Kundargi, R., Goncharov, A., Kharlamova, S., Montoya, J., 2008. In situ thermal diffusivity measurements of $MgSiO_3$ perovskite at lower mantle pressures. In: American Geophysical Union, Fall Meeting 2008, (abstract # MR53A-1730).
Lehmuskero, A., Kuittinen, M., Vahimaa, P., 2007. Refractive index and extinction coefficient dependence of thin Al and Ir films on deposition technique and thickness. Opt. Express 15, 10744–10752.
Lin, J.-F., Watson, H., Vankó, G., Alp, E.E., Prakapenka, V.B., Dera, P., Struzhkin, V.V., Kubo, A., Zhao, J., McCammon, C., Evans, W.J., 2008. Intermediate-spin ferrous iron in lowermost mantle post-perovskite and perovskite. Nat. Geosci. 1, 688–691.
Manga, M., Jeanloz, R., 1997. Thermal conductivioty of corundum and periclase and implications for the lower mantle. J. Geophys. Res. 102, 2999–3008.
Mao, W.L., Shen, G., Prakapenka, V.B., Meng, Y., Campbell, A.J., Heinz, D.L., Shu, J., Hemley, R.J., Mao, H.-K., 2004. Ferromagnesian post-perovskite silicates in the D" layer of the Earth. Proc. Natl. Acad. Sci. U.S.A. 101, 15867–15869.
McCammon, C., Kantor, I., Narygina, O., Rouquette, J., Ponkratz, U., Sergueev, I., Mezouar, M., Prakapenka, V., Dubrovinsky, L., 2008. Intermediate-spin ferrous iron in lower mantle perovskite. Nat. Geosci. 1, 684–687.
Montoya, J.A. et al., in preparation.
Ohta, K., Onoda, S., Hirose, K., Sinmyo, R., Shimizu, K., Sata, N., Ohishi, Y., Yasuhara, A., 2008. The electrical conductivity of post-perovskite in Earth's D″ layer. Science 320, 89–91.
Osako, M., 1991. Thermal diffusivity of $MgSiO_3$ perovskite. Geophys. Res. Lett. 18, 239–242.
Ross, R.G., Andersson, P., Sundqvist, B., Bäckström, G., 1984. Thermal conductivity of solids and liquids under pressure. Rep. Prog. Phys. 47, 1347–1402.
Sherman, D.M., 1991. The high-pressure electronic structure of magnesiowustite (Mg,Fe)O: applications to the physics and chemistry of the lower mantle. J. Geophys. Res. 96, 14299–14312.
Srecec, I., Ender, A., Woermann, E., Gans, W., Jacobsson, E., Eriksson, G., Rosén, E., 1987. Activity-composition relations of the magnesiowüstite solid solution series in equilibrium with metallic iron in the temperature range 1050–1400 K. Phys. Chem. Miner. 14, 492–498.
Xu, Y., Shankland, T.J., Linhardt, S., Rubie, D.C., Langenhorst, F., Klasinski, K., 2004. Thermal diffusivity and conductivity of olivine, wadsleyite and ringwoodite to 20 GPa and 1373 K. Phys. Earth Planet. Interior 143–144, 321–336.
Zerr, A., Boehler, R., 1993. Melting of $(Mg,Fe)SiO_3$-perovskite to 625 kbar: indication of a high melting temperature in the lower mantle. Science 262, 553–555.